

Collision of two black holes: Theoretical framework*

Larry Smarr

Princeton University Observatory, Princeton, New Jersey 08540

Andrej Čadež

Univerza v Ljubljani, Fakulteta za Naravoslovje in Tehnologijo, Odsek za Fiziko, 61000 Ljubljana, Yugoslavia

Bryce DeWitt

Center for Relativity, Department of Physics, University of Texas, Austin, Texas 78712

Kenneth Eppley

Department of Physics and Astronomy University of North Carolina, Chapel Hill, North Carolina 27514

(Received 21 June 1976)

Highly nonspherical time-dependent collisions between black holes may be powerful sources of gravitational radiation. We consider various attempts at estimating the efficiency of the generation of radiation by such collisions. To determine the actual efficiency as well as to understand the details of the dynamical coalescence of black-hole event horizons, we have developed a numerical method for solving the Einstein gravitational field equations in these high-velocity strong-field regions. The head-on collision of two nonrotating vacuum black holes is chosen as an example of our technique. We use the geometrodynamical model of a black hole as an Einstein-Rosen bridge. The initial data to be evolved are the time-symmetric conformally flat data discovered by Misner. A new set of spatial coordinates for these data is derived. Then the general space plus time decomposition of Einstein's equations is presented and specialized to the axisymmetric nonrotating case. Details of the evolution will be given in later papers.

I. INTRODUCTION

Because of the rapid increase in the sensitivity of Weber-type resonant-bar gravitational wave antennas,¹ we may soon be capable of detecting² bursts of gravitational radiation emitted in our galaxy by collisions of black holes or by the nonspherical final collapse of stars. Furthermore, new techniques, such as Doppler tracking of interplanetary spacecraft,³ may let us observe these violent events in the nuclei of distant quasars, galaxies, or globular clusters.⁴ Therefore, it is important to calculate the details of the expected waves. Unfortunately, it is precisely in these situations of strong gravitational field ($R \sim R_{\text{Sch}} = 2GM/c^2$) and fast motion ($v \sim c$) that all known approximation schemes in general relativity fail (see Thorne and Kovács⁵ for a review of existing techniques). What is needed is a method for obtaining highly nonspherical, time-dependent, and physically realistic solutions of the full nonlinear Einstein equations which describe gravitational fields produced by collapse or collision.

Since we could not solve this problem analytically, we developed a numerical method using digital computer programs to integrate the axisymmetric, finite-differenced, Einstein equations. (The restriction of axisymmetry was imposed solely because of limited computer memory and speed. Our techniques can be generalized to the generic case of no spatial symmetry.) In this procedure, we

start with some initial data specified on a space-like hypersurface. Using the 3+1 (space+time) decomposition of spacetime⁶ we then build up both the four-dimensional coordinate system and the Cauchy evolution of the initial data simultaneously. The general theory of how to build a "good" spacetime coordinate system slice by slice will be described elsewhere.⁷ The present paper is the first in a series describing the calculation of a specific spacetime representing the head-on collision of two black holes.

We chose the collision problem as a first "test case" for several reasons. First, the spacetime can be purely vacuum by using Einstein-Rosen bridges⁸ to represent the two black holes. This means we can avoid all the messy hydrodynamics which is needed even in spherical stellar collapse.⁹ Second, an initial data set is known analytically¹⁰ and has been exhaustively analyzed (see Sec. III for references). Third, the spacetime involves many unexplored aspects of highly nonspherical black holes, generation of gravitational waves in time-dependent strong-field regions, and propagation of the waves outward into the wave zone where they can be measured. Fourth, the results of this calculation will be relevant for astrophysics since they will test whether the high efficiencies ($\sim 10\%$) which are usually assumed^{4,11} for conversion of rest mass to gravitational radiation actually occur.

As the computational geometrodynamical tech-

niques become “battle-tested” on this problem, we expect to turn to calculating the full relativistic collapse of stars to form neutron stars or black holes. Thuan and Ostriker¹² have calculated the gravitational radiation expected from nonspherical dust collapses assuming Newtonian physics. Novikov¹³ has pointed out that if pressure is included, the efficiency can be much higher during the “bounce.” Work on the Einstein version of their calculation is now being pursued using our formalism (see Pachner and Teshima,¹⁴ for an alternate approach).

In this paper we first briefly recall the history of the two-body problem in general relativity (Sec. II). Then (Sec. III) we consider the Misner initial data for the collision. We discuss various ideas for estimating upper limits on the radiation efficiency. The original spatial coordinates introduced by Misner are not suited to numerical evolution, so we have devised a new set in terms of which the initial data are given (Sec. IV). The next paper in this series will describe an evolution of the initial data.

II. HISTORY

Almost since the beginning of general relativity, the two-body problem has been a central issue. Early efforts were made by Bach, Weyl, and Levi-Civita to obtain a static axisymmetric two-body solution, but such efforts were doomed to failure. Because of the attractive nature of gravitation, any two-body problem must be time dependent¹⁵ unless there are “singularity struts” present or counterbalancing electromagnetic forces (see, e.g., Cooperstock¹⁶ and Hartle and Hawking¹⁷ for discussions). Since an exact time-dependent solution seems unlikely to be presented, the study of two bodies has mainly been confined to an initial data sheet. Three pioneering approaches to this problem emerged in the 1930’s (see Wheeler¹⁸ for a review): (1) The geometrodynamical model of two masses as non-Euclidean bridges between asymptotically flat spaces was formulated by Einstein and Rosen. (2) The time-symmetric conformally flat initial data with real masses on a Euclidean space were set up by Lichnerowicz.¹⁹ (3) The Einstein-Infeld-Hoffman approximation method for deriving the equations of motion from the field equations was investigated. We will not concern ourselves here with the third alternative, because we are not interested in approximations, but rather in finding a full spacetime representing the collision of two bodies. For the case where the two holes remain in each other’s weak-field region see the beautiful recent work of D’Eath.²⁰ The second method has lain dormant but is currently being revived for studies of nonspherical collapse.²¹ The

rest of our story follows the approach of Einstein and Rosen, brought to fruition by Wheeler, Misner, and their co-workers in the early 1960’s.

In 1960 Misner investigated an analytic set of initial data for the vacuum two-body problem. It was for equal masses and contained two free parameters which set the total mass and initial separation distance of the two throats. Brill and Lindquist followed this up by producing a time-symmetric conformally flat initial data set for N throats in vacuum²² or with electric fields present.²³ They showed, as Lichnerowicz had shown for the “matter” N -body problem, that one recovers the Newtonian potential description if the bodies are far apart. The first attempt at obtaining a numerical solution for the evolution of the initial data was made by Hahn and Lindquist.²⁴ Their work demonstrated the feasibility of this approach and confirmed that each throat behaved much like a single Schwarzschild throat. Unfortunately, they were hampered by a number of problems beyond their control. First, the physical setting was unknown. The notion of black holes and horizons, the area theorems, and the scope of the problem had not yet been defined. Second, the Misner coordinates, while useful for obtaining the initial data, proved disastrous for computer calculations of the far-field region. Third, they were only able to integrate for a very short time into the future of their initial slice. In the late 1960’s DeWitt started a research effort on the feasibility of colliding two black holes on a computer. This led directly to theses by Čadež,⁴⁸ Smarr,³⁰ and Eppley²⁵ on the problem. The results of these theses are reported in this series of papers.

III. MISNER INITIAL DATA

As mentioned above, there are various ways one can choose initial data to represent two black holes. Presumably, the most realistic case would be modeled by the Lichnerowicz approach. There one has two pockets of matter representing two stars initially at rest. One could set up the data so that as the stars started falling toward one another, they would collapse to form black holes on the way. Then the black holes would collide with very complicated hydrodynamics inside the final black hole as the matter coalesced. However, the details of what occurs inside the black holes cannot affect what occurs outside. Therefore, it is equally realistic to use the vacuum Einstein-Rosen model for two black holes which replaces each star with a “throat” joining two separate universes. This is in exact analogy to the well-known procedure followed for a single spherical Schwarzschild

black hole. There the “realistic” model uses only that part of the Kruskal extended manifold outside of the surface of a collapsing star. However, almost all of our knowledge about black-hole physics has come from studying the vacuum solutions (Kerr or Schwarzschild) with their two universes connected by a throat. (See, e.g., Carter.²⁶) Furthermore, we will argue below that if the collision of two black holes is capable of radiating gravitational radiation with a high efficiency, then this radiation will be produced during the coalescence of the horizons. Since this is a nonlocal occurrence involving the entire region around the holes, we may expect that its efficiency will not depend strongly on the details of the initial data. Therefore, we chose to evolve Misner’s initial data because they were the easiest to work with numerically. In the future, we hope to test the dependence of the radiation produced on the initial data by evolving other inequivalent black-hole initial data.²⁷

In general, the initial data for a gravitational field are given on a spacelike hypersurface by two three-dimensional symmetric tensor fields: γ_{ij} , the three-metric, and K_{ij} the extrinsic curvature (see, e.g., O’Murchadha and York²⁸). The γ_{ij} gives the proper distances and angles between any two events lying in the spacelike hypersurface, while K_{ij} tells how the three-surface is embedded in the four-dimensional spacetime. Since the fourth coordinate is time, the extrinsic curvature is essentially the first time derivative of γ_{ij} (see below for details).

Let us now review the Misner¹⁰ initial data. Topologically, they are two Euclidean sheets joined by two throats. Metrically, the two sheets are asymptotically flat universes. The initial data represent either two black holes or a single deformed black hole, depending on the initial separation.²⁹ In either case the initial surface is a moment of time symmetry ($K_{ij}=0$). In order to obtain an analytic solution, one takes for the 3-metric the conformally flat line element

$$ds^2 = a^2 \Psi^4 (d\rho^2 + dz^2 + \rho^2 d\phi^2). \quad (1)$$

As is well known, Ψ must be a solution of $\Delta\Psi=0$, where Δ is the flat-space Laplacian in cylindrical coordinates, in order that the Einstein constraint equations be satisfied. Using techniques familiar from electrostatics, Misner constructed a Ψ which forces an isometry between the upper and lower sheets:

$$\Psi = 1 + \sum_{n=1}^{\infty} \text{csch}(n\mu_0) \left(\frac{1}{+r_n} + \frac{1}{-r_n} \right), \quad (2)$$

$$\pm r_n = \{\rho^2 + [z \pm \coth(n\mu_0)]^2\}^{1/2}.$$

There are two free parameters (a, μ_0) which appear in the line element. One has the dimensions of length (a) and one is dimensionless (μ_0). We have pulled a^2 out of the line element so that the coordinates (ρ, z) are dimensionless. Misner and Lindquist have shown that the parameters (a, μ_0) are related to the physical parameters (M, L), where M is the total mass of the system as measured at spatial infinity and L is the proper distance along the spacelike geodesic connecting the two throats:

$$M = 4a \sum_{n=1}^{\infty} \text{csch}(n\mu_0), \quad (3a)$$

$$L = 2a \left[1 + 2\mu_0 \sum_{n=1}^{\infty} n \text{csch}(n\mu_0) \right]. \quad (3b)$$

Misner,¹⁰ Wheeler,¹⁸ Lindquist,²³ and Brill and Lindquist²² discuss how the two throats distort themselves in a manner suggesting a Newtonian tidal deformation. This is to be expected since the only nonzero components of the four-dimensional Riemann curvature tensor on a vacuum time-symmetric slice are the tidal components ${}^4R_{0i0j}$.³⁰ One can define an interaction energy for this bound system as²³

$$m_{\text{int}} \equiv M - 2m = -4a \sum_{n=1}^{\infty} (n-1) \text{csch}(n\mu_0), \quad (4)$$

$$m = 2a \sum_{n=1}^{\infty} n \text{csch}(n\mu_0),$$

where m is the “bare” mass assigned to each throat. Note that this interaction energy grows more and more negative as $\mu_0 \rightarrow 0$, and becomes the Newtonian binding energy for large separation ($\mu_0 \rightarrow \infty$).

From the work of Hawking³¹ and others, we know that the surfaces of the black holes, the global event horizon, lie outside of the throats. In the initial time-symmetric surface, the throats are minimal surfaces and, thus, marginally trapped surfaces.³² When the holes are close enough together, a new minimal surface appears surrounding the entire system. Just by looking at this initial data sequence then we have a strong indication that the event horizon for the two black holes will merge and form a distorted black hole during an actual evolution. It is important for us to know when such a merging has occurred. Čadež has found the value of μ_0 at which the new minimal surface first appears on the Misner initial data ($\mu_0 = 1.362$) and has calculated its position and area. We shall see in a moment that this enables us to set upper bounds on the amount of radiation which might be produced by the evolution. In Table I, we give values of M , L , L/M , m/M , and m_{int}/M as functions of μ_0 . For reference, our preliminary computer calculations have been carried out from

TABLE I. The values of M , L , L/M , m/M , and n_{int}/M as functions of μ_0 .

μ_0	M	L	L/M	m/M	n_{int}/M
1.0	5.14	9.87	1.92	0.77	-0.53
1.5	2.39	6.58	2.75	0.64	-0.28
2.0	1.27	4.94	3.88	0.58	-0.15
2.5	0.72	3.96	5.50	0.54	-0.09
3.0	0.42	3.33	7.92	0.53	-0.05

initial data with $\mu_0 = 2$.

We can get an estimate of the time required for a collision to occur by solving the Newtonian problem of the free fall of two point particles which start at rest at $t=0$. If we let the initial separation be $L(\mu_0)$ and the total mass be $M(\mu_0)$, then one can integrate the equation of motion to obtain t_{coll} , the time of the "collision", when the separation is $2M$, and $(v/c)_{\text{coll}}$ at that point. These are given in Table II. Although it would seem that L has little to do with Newtonian distances in such strong-field regions, we shall see in paper II that this estimate of free-fall time is within a factor of order unity of the general relativistic value for the coalescence of the surfaces of the black holes. For an illustration of the expected development of the horizon structure see Hawking.³³ As one can see, there are essentially three phases in this evolution. The first is just an in-flight period while the holes are far apart but moving toward each other. The second is when they get close enough to each other that they very rapidly tidally distort one another. The final phase is when they are coalescing. During this last phase one has a single black hole with huge nonspherical deformations.

During each of these phases we expect gravitational radiation to be produced. However, the mechanism is somewhat different in each case. For the in-flight radiation, we can think of the system as two point masses falling toward each other. This gives a time-changing quadrupole moment. As they near each other, their finite dimensions come into play, and we can imagine each hole to have a "quadrupole" moment which changes very rapidly as the holes distort one another. Finally, with the coalescence, one may very well expect a strong burst of radiation as the equatorial sections of the event horizon expand outward to form a spherical black hole. After this big pulse, a long train of "ringing" waves may occur,³⁴ gradually dying out until only a spherical black hole is left surrounded by a region of radiation propagating to infinity.

We can use several techniques to estimate the importance of these phases for producing radiation during a head-on collision. Let us assume

TABLE II. The values of L/M , t_{coll}/M and $(v/c)_{\text{coll}}$ as functions of μ_0 . Here t_{coll} is the time for the two particles to fall together from a separation of L to a separation of $2M$.

μ_0	L/M	t_{coll}/M	$(v/c)_{\text{coll}}$
1.5	2.75	3.20	0.52
2.0	3.88	6.86	0.70
2.5	5.50	12.80	0.80
3.0	7.92	23.30	0.86

that two holes of equal mass m_i are projected inward from infinity with velocity v_∞ . Then by energy conservation

$$2m_i \gamma_\infty = m_f + E_{\text{rad}}, \quad (5)$$

where $\gamma_\infty = (1 - v_\infty^2)^{-1/2}$, m_f is the final mass of the single hole, and E_{rad} is the energy carried off by gravitational radiation. We can combine this with Hawking's theorem³¹ that the total surface area of black holes must increase (assuming cosmic censorship holds),

$$A_1 + A_2 \leq A_f, \quad (6)$$

where $A_i = 16\pi m_i^2$, to obtain an upper limit on the efficiency of radiation, Fig. 1 (Hawking³⁵ for the $v_\infty = 0$ case, Smarr³⁰ for the $v_\infty > 0$ case):

$$\epsilon = E_{\text{rad}} / (2m_i \gamma_\infty) \leq 1 - \frac{1}{\gamma_\infty \sqrt{2}} \rightarrow \begin{cases} 1.00, & v_\infty \rightarrow 1 \\ 0.295, & v_\infty \rightarrow 0 \end{cases} \quad (7)$$

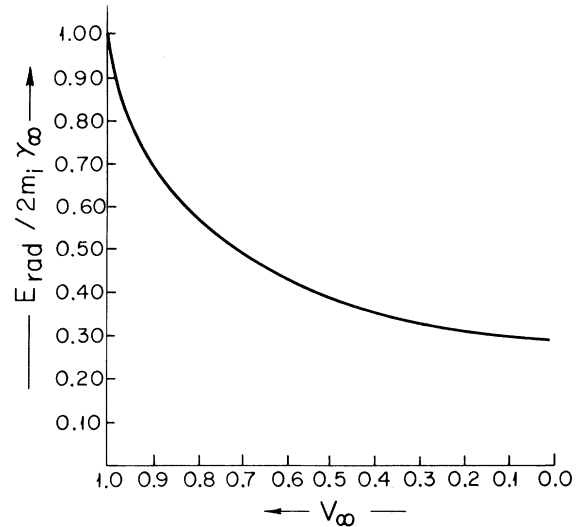


FIG. 1. The upper limit (using the Hawking area increase theorem) on the efficiency of conversion of the energy of two colliding black holes with hyperbolic velocities to gravitational radiation. The initial velocity at infinite separation (v_∞) is plotted horizontally and the efficiency ($E_{\text{rad}}/2m_i\gamma_\infty$) is plotted vertically.

The reason the upper bound on efficiency rises so fast as $v_\infty \rightarrow 1$ is that the colliding black holes become "Lorentz-contracted"³⁷ and appear to be more and more like colliding plane waves.³⁶ Their energy is almost totally bound up in kinetic energy which presumably will be radiated leaving only the "rest mass" in the final black hole. An approximate calculation of the efficiency for the extreme case $v_\infty \approx 1$ indicates that $\epsilon \approx 0.3 - 0.6$.³⁹

For two black holes which are initially bound, upper limits can also be calculated, but they are not quite as stringent since they depend on using the apparent horizons instead of the event horizons. The notion is that the bound system can be approximated by the Misner initial conditions. In such a time-symmetric slice we can measure the area of the minimal surfaces which are the *apparent* horizons. We then use area theorems as before to estimate the radiation. Gibbons and Schutz⁴⁰ carried out this program for the minimal surfaces at the throats. They found that the efficiency must decrease as the holes move together. Unfortunately they made an error in calculating L so their graph must have its scale for (M/L) corrected. (There was no error in their calculation of the efficiency as a function of μ_0 .) The numbers are graphed in Fig. 2. Note that apparent horizons are probably a useful approximation to the event horizon when the holes are far apart ($L/M \gtrsim 10$), but that they become less useful as the holes move together, until a third apparent horizon appears surrounding the other two. Čadež used the area of

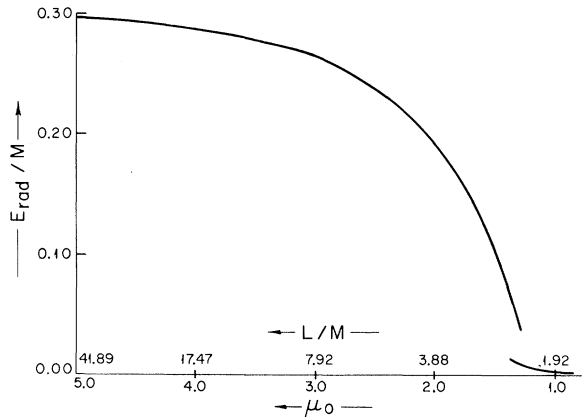


FIG. 2. The upper limit on the efficiency of conversion of total mass into radiation for two bound black holes. Here one assumes the Misner initial data with zero angular momentum. The horizontal scale gives Misner's parameter μ_0 and the initial spacelike separation of the two throats (L) in units of the total mass (M) of the system. The upper curve is based on using the apparent horizons of each hole, while the lower curve is obtained after a third apparent horizon surrounds the other two on the initial slice.

this third surface for $\mu_0 < 1.362$ to place a much tighter limit and it is also plotted.

Going back to the parabolic infall when Hawking gives an upper limit of $E_{\text{rad}} = 0.295Mc^2$, we can estimate the in-flight radiation by calculating the quadrupole moment as a function of time of two mass points falling toward each other starting at rest with infinite separation, and using Newton's law of motion with the force provided by Newton's law of gravity. One then puts the third time derivative of this quadrupole moment into the Landau-Lifshitz⁴¹ expression to obtain the gravitational radiation emitted. The result of this calculation⁴² is $E_{\text{rad}} = 0.02(\mu^2 M)c^2$, where μ is the reduced mass and M is the total mass of the two particles, and where one stops the integration when the separation is $2GM/c^2$. This is only a factor of 2 greater than the fully relativistic calculation of a particle of small mass μ falling into a large mass M black hole.⁴³ Therefore, the Newtonian approximation might be believed as an order-of-magnitude estimate for the gravitational radiation emitted, by two *equal mass* black holes, up to the time when their finite size becomes important. The result is now $E_{\text{rad}} \approx 0.001Mc^2$, a factor of 300 less than Hawking's upper limit. For this reason, we feel that *if* any appreciable amount of radiation is produced by the head-on collision, it will come from the last two phases.

Estimating the radiation from the last two phases is very difficult since all known approximation techniques break down for both strong fields and fast motions. For the second phase, one might use the Mashhoon⁴⁴ calculation for tidal gravitational radiation produced by a neutron star falling into a black hole. If one uses a neutron star of black-hole "density" and extent in Mashhoon's formulas, one comes out with $E_{\text{rad}} \approx 0.01Mc^2$. Even if a pulse of radiation can be formed by the outward moving event horizon, it still must fight the huge gravitational red-shift, as well as avoid being backscattered off the curvature, if it is to escape to infinity. Clearly only an actual solution of the full non-linear, time-dependent, non-spherically-symmetric Einstein equations can settle the question of the efficiency of black-hole collisions for producing gravitational radiation.

We wish to emphasize that the above discussion applies only to the head-on collision case. If the two black holes fall from infinity with a small enough impact parameter they will be able to "capture" each other by emitting gravitational bremsstrahlung radiation and then they will spiral in toward each other by emitting more gravitational radiation³⁸ carrying off both energy and angular momentum.⁴⁵ Finally, they will plunge into each other in a coalescence burst of radiation. Since the non-

zero impact parameter opens up these physically new radiation processes, one might hope for considerably better efficiency than is achieved in the head-on case.

IV. THE SPACETIME METRIC

We will now describe the general technique for constructing a spacetime from a set of initial data. Following Dirac and Arnowitt, Deser, and Misner,⁶ we decompose spacetime into a set of spacelike hypersurfaces or slices S_t . The particular slicing we choose defines "time" as being that spacetime scalar function t which is constant on each S_t . The spatial coordinates can be defined by threading a congruence of curves through the slices, with each member of the congruence labeled by three numbers. This coordinate congruence may or may not be normal to the slices. Thus, an event in spacetime has coordinates (t, x_i) , where t is the value given by the S_t containing the event and x_i are the labels of the coordinate curve passing through the event.

This great flexibility in choice of spacetime coordinates is a consequence of the general covariance of the Einstein equations. As we will see in later papers in this series, it is essential to make full use of this coordinate freedom if we are going to be able to successfully evolve a dynamic black-hole spacetime. To code the coordinate freedom explicitly into the Einstein equations, one introduces the lapse function α and the shift vector β_i (see, e.g., Wheeler⁴⁶). The lapse function controls the choice of slicing since it gives the proper time $d\tau$ along the normals from S_t to S_{t+dt} :

$$d\tau = \alpha(x_i)dt. \quad (8)$$

For example, if $\alpha = 1$ everywhere on the slice then the S_t are geodesically parallel. The shift vector β_i is nonzero if the coordinate congruence is not orthogonal to the S_t . In this case, β_i is the 3-vector joining two events in S_{t+dt} : One is the event reached by the curve normal to S_t through the event (t, x_i) , the other is the event $(t+dt, x_i)$ reached by the coordinate line through (t, x_i) .

One can now write down the 4-metric ${}^4g_{\mu\nu}$ in terms of α , β_i , and γ_{ij} , where γ_{ij} is the 3-metric on S_t :

$${}^4g_{\mu\nu} = \begin{pmatrix} -\alpha^2 + \beta_k \beta^k & \beta_j \\ \beta_i & \gamma_{ij} \end{pmatrix}. \quad (9)$$

Inserting this form into the 10 Einstein equations for vacuum (${}^4G_{\mu\nu} = 0$) leads to four constraint equations (the Hamiltonian and momentum constraints),

$$H \equiv R + K^2 - K_{ij}K^{ij} = 0, \quad (10a)$$

$$H_i \equiv D_i K - D_j K^j_i = 0, \quad (10b)$$

and six second order in time evolution equations (split into six pairs of first-order equations),

$$\partial_t \gamma_{ij} = -2\alpha K_{ij} + D_i \beta_j + D_j \beta_i, \quad (11a)$$

$$\begin{aligned} \partial_t K_{ij} = & -2\alpha K_{i\ell}K^{\ell}_j + \alpha K_{\ell}^{\ell}K_{ij} \\ & + \alpha R_{ij} - D_i D_j \alpha + \beta^{\ell} D_{\ell} K_{ij} \\ & + K_{i\ell} D_j \beta^{\ell} + K_{\ell j} D_i \beta^{\ell}. \end{aligned} \quad (11b)$$

Here K_{ij} is the extrinsic curvature tensor which tells how the S_t is bent in the surrounding spacetime and D_i is the spatial covariant derivative. In summary, our plan is to choose initial data (γ_{ij}, K_{ij}) which satisfy the constraint equations (10). We then choose the lapse (α) and the shift (β_i) which extend our coordinates to the next slice. Using $(\alpha, \beta, \gamma_{ij}, K_{ij})$ in the evolution equations (11), we propagate (γ_{ij}, K_{ij}) to the new S_t and then repeat the whole process. For a more complete derivation and discussion of the geometry and kinematics of the 3+1 (space and time) formalism see Smarr³⁰ and Smarr and York.⁷

Let us now specialize to the case of axisymmetry. This restriction means that all gravitational field variables depend at most on two space variables (x_1, x_2) and time (t) . We will denote the azimuthal angle by ϕ . It is convenient to use the standard (z, ρ) coordinates as our base variables because they are well-defined everywhere. Unfortunately, the boundaries of the two-black-hole spacetime do not lie along lines of constant (z, ρ) . For this reason it is useful to introduce two new coordinates (η, ξ) with η a "radial" coordinate and ξ and "angular" coordinate. Figure 3 sketches the desired properties of η and ξ : They should be "quasi-spherical" both near each throat and far from the holes. These two demands mean (η, ξ) are singular at the saddle point $(z, \rho) = (0, 0)$. A particular set of these coordinates is described in Appendix A and compared with Misner's coordinates which do not have the desired properties. In any case, because of the general covariance of Einstein's equations, we may use whichever set of labels (x_1, x_2)

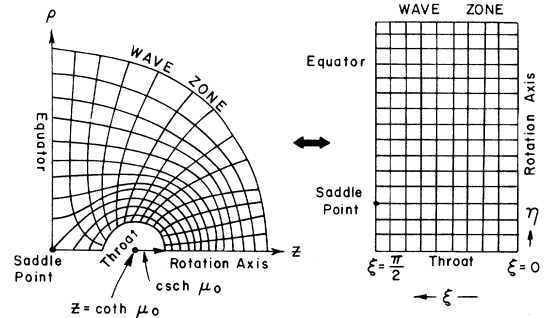


FIG 3. Schematic representation of the coordinate grid for two black holes.

we wish and then transform between them in the standard fashion.

The initial metric was chosen to be time symmetric and conformally flat [Eq. (1)]. Since we know the conformal factor Ψ analytically [Eq. (2)], we shall always factor Ψ^4 out of the metric and evaluate its derivatives analytically. This means we shall evolve only the conformal metric in keeping with York's emphasis.⁴⁷ Because of the coordinate transformation described above, we know that $\rho^2 = \rho^2(\eta, \xi)$ analytically so we shall always factor it out of the $d\phi^2$ term. Now in general the symmetric γ_{ij} has six independent entries. However, for this problem there is no rotation involved so $\gamma_{\phi\rho}$ and $\gamma_{\phi z}$ can be set equal to zero for all time. This leaves us with four functions in the metric tensor,

$$\gamma_{ij} = \Psi^4 \begin{pmatrix} A & C & 0 \\ C & B & 0 \\ 0 & 0 & \rho^2 D \end{pmatrix}, \quad (12)$$

with the ordering (z, ρ, ϕ) or (η, ξ, ϕ) . The first Einstein equation (11a) shows that K_{ij} will have the same number of components as γ_{ij} , so we define its entries as

$$K_{ij} = \Psi^4 \begin{pmatrix} K_A & K_C & 0 \\ K_C & K_B & 0 \\ 0 & 0 & \rho^2 K_D \end{pmatrix}. \quad (13)$$

The eight Einstein differential equations (11) we need to difference are now of the form (with $\beta^i = 0$)

$$\begin{aligned} \partial_t A &= -2\alpha K_A, \\ \partial_t K_A &= \alpha(AB - C^2)^{-1} [K_A(-BK_A + AK_B + 2CK_C) - 2AK_C^2] \\ &\quad + \alpha DK_A K_B + \Psi^{-4}(\alpha R_{zz} - \alpha|_{zz}), \\ \dots, \end{aligned} \quad (14)$$

where the Ψ^4 conformal factor is taken out of the Christoffel symbols and Ricci tensor by the standard formulas. The explicit form of the right-hand side of these equations is given in Appendix B. These evolution equations must be supplemented by equations specifying the lapse and shift. In Eq. (14) we have specified $\beta_i = 0$, which demands that our coordinate lines $(x_1, x_2, \phi) = \text{constant}$ be normal to the S_t . The lapse has been left free. Its specification and the use of these equations to obtain a collision spacetime are the subject of paper II.

ACKNOWLEDGMENTS

We gratefully acknowledge many useful conversations with colleagues and friends. For encourage-

ment and advice we are especially indebted to Dieter Brill, Charles Misner, Jerry Ostriker, John Wheeler, and James York. Helpful remarks on the manuscript were made by Nicholas Woodhouse and William Press. We also appreciate the hospitality and support of the Princeton University Physics Department and the University of Maryland Physics Department. We thank Dennis Sciama for providing the stimulating atmosphere at the Astrophysics Department, Oxford University, where parts of this paper were revised.

APPENDIX A

A desirable property of any coordinate system is that it be adapted to the physical symmetries of a problem. For the two black holes this means we wish the coordinates to be quasospherical near the throats of the Einstein-Rosen bridges as well as far away from the holes in the wave zone. To construct such coordinates from the natural cylindrical (z, ρ) coordinates, we use a standard method from complex variables. Choose a complex analytic function $\chi(\zeta)$ where $\zeta = z + i\rho$. Then the real and imaginary parts of χ are the new coordinate lines.

For instance, to obtain spherical coordinates one defines

$$\chi(z + i\rho) = \ln(\zeta). \quad (A1)$$

The logarithm function places a pole at the origin. The real and imaginary parts define a radial coordinate η and an angular coordinate ξ by

$$\eta = \text{Re}(\chi) = \frac{1}{2} \ln(\rho^2 + z^2) = \ln R, \quad (A2)$$

$$\xi = \text{Im}(\chi) = \tan^{-1}(\rho/z) = \theta, \quad (A3)$$

where R and θ are the standard polar coordinates. Note that the logarithm in χ leads to a logarithmic radial coordinate.

Let us examine Misner's choice of coordinates from this viewpoint. His χ is the superposition of two equal but opposite poles at $z = \pm \coth \mu_0 = \pm z_0$,

$$\chi(\zeta) = \ln(\zeta + \zeta_0) - \ln(\zeta - \zeta_0), \quad (A4)$$

where $\zeta_0 = (z_0, 0)$. By an easy calculation using $\coth^{-1} \eta = \frac{1}{2} \ln[(\eta + 1)/(\eta - 1)]$, one finds that

$$\eta = \text{Re} \chi, \quad \xi = \text{Im} \chi \quad (A5)$$

are just the bispherical coordinates used by Misner and Lindquist:

$$\coth \eta = (\rho^2 + z^2 + z_0^2)/(2zz_0), \quad (A6)$$

$$\coth \xi = (\rho^2 + z^2 - z_0^2)/(2\rho z_0).$$

To transform the initial data from the cylindrical

coordinates given in Eq. (1), we use the Cauchy-Riemann equations

$$\begin{aligned}\frac{\partial \eta}{\partial z} &= \frac{\partial \xi}{\partial \rho}, \quad \frac{\partial \eta}{\partial \rho} = -\frac{\partial \xi}{\partial z}, \\ \frac{\partial^2 \eta}{\partial z^2} &= -\frac{\partial^2 \eta}{\partial \rho^2} = \frac{\partial^2 \xi}{\partial \rho \partial z}, \\ \frac{\partial^2 \eta}{\partial z \partial \rho} &= \frac{\partial^2 \xi}{\partial \rho^2} = -\frac{\partial^2 \xi}{\partial z^2}\end{aligned}\quad (\text{A7})$$

and the Jacobian of the two coordinate systems

$$J = \left| \frac{d\chi}{d\xi} \right|^2 = \left(\frac{\partial \eta}{\partial \rho} \right)^2 + \left(\frac{\partial \eta}{\partial z} \right)^2. \quad (\text{A8})$$

This yields the initial metric in the new coordinates

$$ds^2 = a^2 \Psi^4 \left(\frac{d\eta^2 + d\xi^2}{J} + \rho^2 d\phi^2 \right), \quad (\text{A9})$$

$$\rho = \rho(\eta, \xi), \quad J = J(\eta, \xi), \quad \Psi = \Psi(\eta, \xi).$$

For Misner's χ , Eq. (A4), we have in particular

$$\begin{aligned}J &= (\cosh \eta - \cos \xi)^2 / z_0^2, \\ \rho &= z_0 \sin \xi / (\cosh \eta - \cos \xi),\end{aligned}\quad (\text{A10})$$

and factoring out J^{-1} we find the line element in Misner-Lindquist form:

$$\begin{aligned}ds^2 &= a^2 \tilde{\Psi}^4 (d\eta^2 + d\xi^2 + \sin^2 \xi d\phi^2), \\ \tilde{\Psi}^4 &= \Psi^4 J^{-1}.\end{aligned}\quad (\text{A11})$$

The same procedure can be applied to any other choice of χ . We have chosen equal poles of the same sign plus higher multipoles (see Čadež⁴⁸):

$$\begin{aligned}\chi(\xi) &= \frac{1}{2} [\ln(\xi + \xi_0) + \ln(\xi - \xi_0)] \\ &+ \sum_{n=1}^{\infty} C_n \left(\frac{1}{(\xi_0 + \xi)^n} + \frac{1}{(\xi_0 - \xi)^n} \right).\end{aligned}\quad (\text{A12})$$

The C_n are chosen by a least-squares technique to make the initial throats

$$(z_{\text{th}} \pm z_0)^2 + \rho_{\text{th}}^2 = \text{csch}^2 \mu_0 \quad (\text{A13})$$

lie on an $\eta = \text{constant}$ coordinate line. The resulting coordinate lines (η, ξ) are shown as a function of (z, ρ) in Fig. 4. The important difference between our coordinates (A12) and Misner's is that the conformal map for Misner breaks down $|d\chi/d\xi| \rightarrow 0$ as $\rho, z \rightarrow \infty$, whereas for ours it breaks down as $\rho, z \rightarrow 0$. This is why Misner's coordinates look so distorted [see Fig. 2(b) of Čadež⁴⁸] as one gets farther away from the central region (squares are no longer mapped onto squares). For our system one only has the central saddle point to worry about (see Fig. 4), since only its neighboring squares are distorted.

We evolve the (z, ρ) metric components (e.g., A

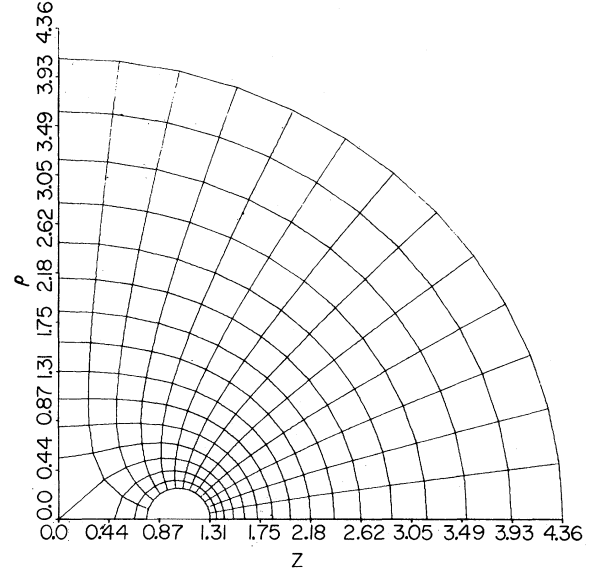


FIG. 4. Actual grid chosen with 14 angular zones and 23 radial zones.

$= \gamma_{zz} / \Psi^4$) because they are defined everywhere. On the other hand, we evaluate these metric components at the “natural” (η, ξ) grid points. Then when we difference a derivative such as $\partial_\rho A$ we use the chain rule

$$\begin{aligned}\partial_\rho &= \eta_{,\rho} \partial_\eta + \xi_{,\rho} \partial_\xi \\ &= \eta_{,\rho} \partial_\eta + \eta_{,z} \partial_\xi,\end{aligned}$$

where we have used (A7). Since the (η, ξ) coordinate grid is derived by using equal grid spacing of $(\Delta\eta, \Delta\xi)$ (see Fig. 3), we can use the standard second-order accurate center differences to represent ∂_η and ∂_ξ ,

$$\begin{aligned}\partial_\eta H_{i,j} &= (H_{i+1,j} - H_{i-1,j}) / (2\Delta\eta), \\ \partial_\xi H_{i,j} &= (H_{i,j+1} - H_{i,j-1}) / (2\Delta\xi), \\ \partial_{\eta\eta} H_{i,j} &= (H_{i+1,j} - 2H_{i,j} + H_{i-1,j}) / (\Delta\eta)^2, \\ \partial_{\xi\xi} H_{i,j} &= (H_{i,j+1} - 2H_{i,j} + H_{i,j-1}) / (\Delta\xi)^2, \\ \partial_{\eta\xi} H_{i,j} &= \frac{H_{i+1,j+1} - H_{i+1,j-1} - H_{i-1,j+1} + H_{i-1,j-1}}{4\Delta\eta\Delta\xi},\end{aligned}$$

where $H_{i,j}$ is a function on the (η, ξ) grid. That is, if the throat is on the coordinate line $\eta = \eta_0$, then

$$H_{i,j} = H[(i * \Delta\eta) + \eta_0, j * \Delta\xi].$$

To obtain the values of functions on the other side of the boundaries in Fig. 3, we use the symmetries of the problem. For details see Čadež,⁴⁸ Eppley,²⁵ and Smarr.³⁰

It is important to remember that our grid stays

fixed through the entire calculation. The metric components are regarded as functions defined over the grid, which vary in time. At a given time one can plug in the appropriate $(\Delta\eta, \Delta\xi)$ or $(\Delta z, \Delta\rho)$ to a metric component and read off the proper distance between two points on the mesh. For instance, as the holes fall together, our grid lines do not get bunched up between the throat and the saddle; rather the metric function $A = \gamma_{zz}/\Psi^4$ will drop from unity toward zero in this region, implying that the proper distance $\Psi^2 \sqrt{A} \Delta z$ is becoming smaller there.

APPENDIX B

Starting with the metric tensor from [Eq. (12)] and the extrinsic curvature from [Eq. (13)], we evaluate the right-hand sides of the Einstein evolution equations (for the full details see Eppley²⁵). The nonzero contravariant metric components $\gamma^{ij} = \Psi^{-4} f^{ij}$ are given by

$$f^{zz} = B\delta, \quad f^{z\rho} = f^{\rho z} = -C\delta, \quad f^{\rho\rho} = A\delta, \quad f^{\phi\phi} = D^{-1}\rho^{-2}, \quad (B1)$$

with $\delta \equiv (AB - C^2)^{-1}$. Assuming that we have formed the first and second spatial differences of A, B, C, D

$$\begin{aligned} R_{zz} = & -\frac{1}{2}f^{\rho\rho}[A_{,\rho\rho} - 2C_{,\rho z} + B_{,zz} - A_{,\rho}G_{z\rho}^z - B_{,z}G_{\rho z}^\rho + (2C_{,\rho} - B_{,z})G_{zz}^z + B_{,\rho}G_{zz}^\rho] \\ & + \frac{1}{2}[-D_{,zz}/D + \frac{1}{2}(D_{,z}/D)^2 + (D_{,z}/D)G_{zz}^z + (D_{,\rho}/D + 2/\rho)G_{zz}^\rho] \\ & - 2\Psi^{-1}(\Psi_{,zz} + Af^{ij}\Psi_{,ij}) + 2\Psi^{-2}(3\Psi_{,z}^2 - Af^{ij}\Psi_{,i}\Psi_{,j}), \end{aligned} \quad (B6)$$

where $\Psi_{,ij} = \Psi_{,ij} - G_{ij}^k \Psi_{,k}$. Finally, the Ricci scalar R is formed by contraction $R = \gamma^{ij} R_{ij}$. Given the metric coefficients, full Christoffel symbols, and Ricci components at each point on the grid, one solves for the lapse α numerically (for instance, $\Delta\alpha - R\alpha = 0$ for maximal slicing—paper II) and then forms its Hessian $\alpha_{,ij} = \alpha_{,ij} - \Gamma_{ij}^k \alpha_{,k}$. With these and the components of K_{ij} we now evaluate the right-hand side of the finite-differenced evolution equations (14). These equations must be modified on the axis ($\rho=0$) by the use of L'Hospital's rule to remove any terms of the form $0/0$. For example, in Eq. (B6) for R_{zz} the term $\rho^{-1}G_{zz}^\rho$ is replaced by

$$\rho^{-1}G_{zz}^\rho \rightarrow \partial_\rho G_{zz}^\rho. \quad (B7)$$

In our first computer calculations, the emphasis was on demonstrating the possibility of evolving the nonspherical Einstein equations by finite-difference techniques. As a result, we were not as much concerned about the details of the numerical techniques used as about obtaining an evolution. For this reason, we took what we

to represent the z and ρ derivatives (see Appendix A), we proceed to construct the conformal Christoffel symbols:

$$G_{jk}^i = \frac{1}{2}f^{il}(f_{ik,j} + f_{jl,k} - f_{jk,l}). \quad (B2)$$

The nonzero ones are $G_{zz}^z, G_{\rho\rho}^\rho, G_{\rho z}^z, G_{z\rho}^\rho, G_{\phi\phi}^\phi$ with a representative example being

$$G_{\rho\rho}^z = \frac{1}{2}(2f^{zz}C_{,\rho} - f^{zz}B_{,z} + f^{z\rho}B_{,\rho}). \quad (B3)$$

The Christoffel symbols of the full metric γ_{ij} may now be found using the formula for conformally related metrics (see, e.g., Hawking and Ellis⁴⁹). This will yield, for instance,

$$\Gamma_{\rho\rho}^z = G_{\rho\rho}^z - 2\Psi^{-1}B(f^{zz}\Psi_{,z} + f^{z\rho}\Psi_{,\rho}). \quad (B4)$$

Using these we can now construct the four Ricci tensor components $R_{zz}, R_{z\rho} = R_{\rho z}, R_{\rho\rho}, R_{\phi\phi}$. Again splitting off the conformal factor pieces (Hawking and Ellis) and writing the conformal part of the Ricci tensor, we have

$$\begin{aligned} R_{ij} = & -\gamma^{kl}(f_{ij,kl} + f_{kl,ij} - f_{kj,il} - f_{li,kj}) \\ & -\gamma^{kl}\gamma_{mn}(G_{kl}^m G_{ij}^n - G_{kj}^m G_{il}^n). \end{aligned} \quad (B5)$$

For instance,

felt was the simplest straightforward approach: Use the differential equations in the standard geometric Hamiltonian form [Eqs. (11a) and (11b)] and use first- or second-order accurate finite-difference approximations for the space and time derivatives. With the right-hand side of the evolution equations [Eq. (14)] evaluated, the first time derivatives were approximated by first-order accurate finite difference:

$$\partial_t H_{i,j} \equiv (H_{i,j}^{t+\Delta t} - H_{i,j}^t)/\Delta t \quad (B8)$$

where $H_{i,j}$ is $A, B, C, D, K_A, K_B, K_C$, or K_D at the (i, j) grid point.

As related in paper II, this scheme did enable us to obtain an evolution. However, the solution of these finite-difference equations contains a numerical instability of the static type common to such forward time difference, center space difference schemes (see, e.g., Roache⁵⁰). A later paper will describe the instability and show how to avoid it by using a more sophisticated differencing scheme.

- *Work supported in part by N. S. F. under Grant No. GP-32039 to the University of Texas at Austin, and Grants Nos. GP-30799X and MPS-74-18470 to Princeton University.
- ¹J. Weber, *Phys. Rev.* **117**, 307 (1960).
 - ²S. P. Boughn, W. M. Fairbank, M. S. McAshan, H. J. Paik, R. C. Taber, T. P. Bernat, D. G. Blair, and W. O. Hamilton, *Gravitational Radiation and Gravitational Collapse*, proceedings of the IAU Symposium 64 edited by C. DeWitt-Morette (Reidel, Dordrecht, 1974).
 - ³F. B. Estabrook and H. D. Wahlquist, *Gen. Relativ. Gravit.* **6**, 439 (1975).
 - ⁴K. S. Thorne and V. B. Braginsky, *Astrophys. J. Lett.* **204**, L1 (1976).
 - ⁵K. S. Thorne and S. J. Kovács, *Astrophys. J.* **200**, 245 (1975).
 - ⁶R. Arnowitt, S. Deser, and C. W. Misner, *Gravitation: An Introduction to Current Research*, edited by L. Witten (Wiley, New York, 1962); P. A. M. Dirac, *Proc. R. Soc. London* **A246**, 333 (1958).
 - ⁷L. Smarr and J. W. York, Jr., paper in preparation.
 - ⁸A. Einstein and N. Rosen, *Phys. Rev.* **48**, 73 (1935).
 - ⁹M. M. May and R. H. White, *Phys. Rev.* **141**, 1232 (1966).
 - ¹⁰C. W. Misner, *Phys. Rev.* **118**, 1110 (1960).
 - ¹¹W. H. Press and K. S. Thorne, *Annu. Rev. Astron. Astrophys.* **10**, 335 (1972).
 - ¹²T. X. Thuan and J. P. Ostriker, *Astrophys. J. Lett.* **191**, L105 (1974).
 - ¹³I. D. Novikov, *Sov. Astron.* **19**, 398 (1976).
 - ¹⁴J. Pachner and R. Teshima, *Can. J. Phys.* **51**, 745 (1973).
 - ¹⁵H. Muller zum Hagen and H. J. Seifert, *Int. J. Theor. Phys.* **8**, 443 (1973).
 - ¹⁶F. I. Cooperstock, *Gen. Relativ. Gravit.* **6**, 91 (1975).
 - ¹⁷J. B. Hartle and S. W. Hawking, *Commun. Math. Phys.* **26**, 87 (1972).
 - ¹⁸J. A. Wheeler, *Rev. Mod. Phys.* **33**, 63 (1961).
 - ¹⁹A. Lichnerowicz, *J. Math. Pure Appl.* **23**, 37 (1944).
 - ²⁰P. D. D'Eath, *Phys. Rev. D* **12**, 2183 (1975).
 - ²¹T. Criss, Ph.D. thesis, Univ. of Texas at Austin, 1975 (unpublished).
 - ²²D. Brill and R. W. Lindquist, *Phys. Rev.* **131**, 471 (1963).
 - ²³R. W. Lindquist, *J. Math. Phys.* **4**, 938 (1963).
 - ²⁴S. G. Hahn and R. W. Lindquist, *Ann. Phys. (N.Y.)* **29**, 304 (1964).
 - ²⁵K. R. Eppley, Ph.D. thesis, Princeton University, 1975 (unpublished).
 - ²⁶B. Carter, in *Black Holes*, edited by C. DeWitt and B. S. DeWitt (Gordon and Breach, New York, 1973).
 - ²⁷D. Brill and R. W. Lindquist, *Phys. Rev.* **131**, 471 (1963); A. Čadež, *Ann. Phys. (N.Y.)* **91**, 58 (1975); L. Smarr and B. S. DeWitt, *Bull. Am. Phys. Soc.* **18**, 643 (1973).
 - ²⁸N. O'Murchadha and J. W. York, Jr., *Phys. Rev. D* **10**, 428 (1974).
 - ²⁹A. Čadež, *Ann. Phys. (N.Y.)* **83**, 449 (1974).
 - ³⁰L. Smarr, Ph.D. thesis, University of Texas at Austin, 1975 (unpublished).
 - ³¹S. W. Hawking, in *Black Holes*, edited by C. DeWitt and B. S. DeWitt (Gordon and Breach, New York, 1973).
 - ³²G. W. Gibbons, *Commun. Math. Phys.* **27**, 87 (1972).
 - ³³Ref. 31, p. 35.
 - ³⁴W. H. Press, *Astrophys. J. Lett.* **170**, L105 (1971); C. J. Goebel, *Astrophys. J. Lett.* **172**, L95 (1972).
 - ³⁵S. W. Hawking, *Phys. Rev. Lett.* **26**, 1344 (1971).
 - ³⁶K. A. Khan and R. Penrose, *Nature* **229**, 185 (1971); P. Szekeres, *J. Math. Phys.* **13**, 286 (1972).
 - ³⁷F. A. E. Pirani, *Proc. R. Soc. London* **A252**, 96 (1959).
 - ³⁸Ya. B. Zel'dovich and M. A. Podvrets, *Sov. Astron.* **9**, 742 (1966).
 - ³⁹L. Smarr, 1976 (unpublished).
 - ⁴⁰G. W. Gibbons and B. F. Schutz, *Mon. Not. R. Astron. Soc.* **159**, 41P (1972).
 - ⁴¹L. D. Landau and E. M. Lifshitz, *The Classical Theory of Fields* (Pergamon, London, 1951).
 - ⁴²F. J. Zerilli, *Phys. Rev. D* **2**, 2141 (1970).
 - ⁴³M. Davis, R. Ruffini, W. H. Press, and R. H. Price, *Phys. Rev. Lett.* **27**, 1466 (1971).
 - ⁴⁴B. Mashhoon, *Astrophys. J.* **185**, 83 (1973).
 - ⁴⁵P. C. Peters and J. Mathews, *Phys. Rev.* **131**, 435 (1963).
 - ⁴⁶J. A. Wheeler, in *Relativity, Groups, and Topology*, edited by C. DeWitt and B. DeWitt (Gordon and Breach, New York, 1964).
 - ⁴⁷J. W. York, *Phys. Rev. Lett.* **28**, 1082 (1972).
 - ⁴⁸A. Čadež, Ph.D. thesis, University of North Carolina at Chapel Hill, 1971 (unpublished).
 - ⁴⁹S. W. Hawking and G. F. R. Ellis, *The Large Scale Structure of Space-Time* (Cambridge Univ. Press, London, 1973), p. 42.
 - ⁵⁰P. Roache, *Computational Fluid Dynamics* (Hermosa, Albuquerque, N. M., 1972), p. 34.